Histochemistry and Cell Biology
https://doi.org/10.1007/s00418-024-02316-7

ORIGINAL PAPER

MEIKIN expression and its C-terminal phosphorylation by PLK1 is closely related the metaphase–anaphase transition by affecting cyclin B1 and Securin stabilization in meiotic oocyte

Li-Hua Fan[1,2,3,4] · Shu-Tao Qi[2,5] · Zhen-Bo Wang[2,4] · Ying-Chun Ouyang[2] · Wen-Long Lei[2,4] · Yue Wang[2,4] · Ang Li[1,2,3] · Feng Wang[1,2,3] · Jian Li[2] · Li Li[2,4] · Yuan-Yuan Li[2] · Yi Hou[2] · Heide Schatten[6] · Wei-Hua Wang[5] · Qing-Yuan Sun[1,2,3,4] · Xiang-Hong Ou[1,3]

Accepted: 22 July 2024

Abstract

Oocyte meiotic maturation failure and chromosome abnormality is one of the main causes of infertility, abortion, and diseases. The mono-orientation of sister chromatids during the first meiosis is important for ensuring accurate chromosome segregation in oocytes. MEIKIN is a germ cell-specific protein that can regulate the mono-orientation of sister chromatids and the protection of the centromeric cohesin complex during meiosis I. Here we found that MEIKIN is a maternal protein that was highly expressed in mouse oocytes before the metaphase I (MI) stage, but became degraded by the MII stage and dramatically reduced after fertilization. Strikingly, MEIKIN underwent phosphorylation modification after germinal vesicle breakdown (GVBD), indicating its possible function in subsequent cellular event regulation. We further showed that MEIKIN phosphorylation was mediated by PLK1 at its carboxyl terminal region and its C-terminus was its key functional domain. To clarify the biological significance of meikin degradation during later stages of oocyte maturation, exogenous expression of MEIKIN was employed, which showed that suppression of MEIKIN degradation resulted in chromosome misalignment, cyclin B1 and Securin degradation failure, and MI arrest through a spindle assembly checkpoint (SAC)-independent mechanism. Exogenous expression of MEIKIN also inhibited metaphase II (MII) exit and early embryo development. These results indicate that proper MEIKIN expression level and its C-terminal phosphorylation by PLK1 are critical for regulating the metaphase–anaphase transition in meiotic oocyte. The findings of this study are important for understanding the regulation of chromosome segregation and the prevention meiotic abnormality.

Keywords MEIKIN · SAC · Cyclin B1 · Securin · PLK1

Li-Hua Fan and Shu-Tao Qi contributed equally.

✉ Wei-Hua Wang
wangweihua11@yahoo.com

✉ Qing-Yuan Sun
sunqy@gd2h.org.cn

✉ Xiang-Hong Ou
ouxianghong2003@163.com

[1] Fertility Preservation Laboratory, Reproductive Medicine Center, Guangdong Second Provincial General Hospital, Guangzhou 510317, China

[2] State Key Laboratory of Stem Cell and Reproductive Biology, Institute of Zoology, Chinese Academy of Sciences, Beijing 100101, China

[3] Guangdong-Hong Kong Metabolism & Reproduction Joint Laboratory, Guangdong Second Provincial General Hospital, Guangzhou 510317, China

[4] University of Chinese Academy of Sciences, Beijing 100101, China

[5] Key Laboratory of Major Obstetrics Diseases of Guangdong Province, The Third Affiliated Hospital of Guangzhou Medical University, Guangzhou 510150, China

[6] Department of Veterinary Pathobiology, University of Missouri, Columbia, MO 65211, USA

Published online: 02 August 2024

Abbreviations

ACA	Anti-centromere antibody
APC/C	Anaphase promoting complex
GV	Germinal vesicle
GVBD	Germinal vesicle breakdown
IBMX	3-Isobutyl-1-methylxanthine
MI	Metaphase I
MII	Metaphase II
PBE	Polar body extrusion
SAC	Spindle assembly checkpoint

Introduction

Meiosis is a special form of cell division, which comprises DNA replication only once followed by two rounds of consecutive chromosome segregation (meiosis I and meiosis II). During meiosis I homologous chromosomes separate, while the sister chromatids are still attached to each other. Finally, sister chromatids separate during meiosis II (Lee and Orr-Weaver 2001; Petronczki et al. 2003). Through meiosis, the diploid parent cells produce haploid gametes. However, chromosome separation, especially in mammalian oocyte meiosis, is a very error-prone process, and any error in this process can lead to aneuploidy. In clinical practice, chromosome aneuploidy is an important cause of infertility, abortion, and diseases (Hassold and Hunt 2001; Jones and Lane 2013; Mihajlović and FitzHarris 2018). To ensure the accuracy of chromosome segregation, a specific set of strict regulatory mechanisms have been developed for meiosis. During meiosis I, homologous chromosomes are paired and recombined to form chiasmata, and sister chromatids are held together by the cohesin complex. Then homologous chromosomes are captured by microtubules emanating from the opposite spindle poles, while the sister chromatids are captured as a unit by microtubules emanating from the same pole. The specific connections between sister chromatids and microtubules is called mono-orientation (Marston and Amon 2004; Musacchio and Salmon 2007). Under the tension of spindle microtubules, homologous chromosomes align at the spindle equator. This process is orchestrated by the spindle assembly checkpoint (SAC). Once an error in the attachment between kinetochores and microtubules occurs, SAC is activated, which further inactivates its downstream anaphase promoting complex (APC/C). The APC/C complex is an E3 ubiquitin ligase that mediates the ubiquitination and degradation of substrates. Cyclin B1 and Securin are two key substrates for the APC/C complex during meiosis. Cyclin B1 is a regulatory subunit of CDK1 and plays an important role in the initiation and termination of meiosis. Securin is an inhibitor of the protease, Separase, which hydrolyzes the cohesin complex and opens the chiasmata between chromosomes. In the case of SAC activation, the activity of the APC/C complex is inhibited. As a result, cyclin B1 and Securin cannot be degraded and their high levels are maintained. Then CDK1 remains highly active and homologous chromosomes cannot segregate, which prevents the onset of anaphase until all chromosomes are properly aligned (Li et al. 2019; Musacchio and Salmon 2007; Peters 2006; Sun and Kim 2012).

The mono-orientation of sister chromatids is a unique feature of meiosis I and is indispensable for accurate step-by-step chromosome segregation. Researchers have always been interested in this topic concerning how sister chromatids as a unit are attached by the microtubules from the same pole. It has been found that there is a key protein to regulate the mono-orientation of sister chromatids in yeast (Katis et al. 2004; Lee et al. 2004; Sullivan and Morgan 2007; Yokobayashi and Watanabe 2005), but it is little known in mammals. Recently, scientists screened this protein by yeast two-hybridization and named it MEIKIN (meiosis-specific kinetochore protein) (Kim et al. 2015). MEIKIN interacts with CENP-C and is localized at centromeres. MEIKIN can recruit PLK1 to regulate mono-orientation of sister kinetochores, and can recruit Shugoshin to protect the cohesin complex at centromeres (Kim et al. 2015). After depletion of MEIKIN, both male and female mice are completely infertile. These results indicate that meikin protein plays a very important role in meiosis. Although we have some understanding of the important functions of the MEIKIN protein in meiosis, there are still questions to be further clarified. According to the literature, MEIKIN loses its localization on centromeres during meiosis II (Kim et al. 2015). Here we have conducted a series of cellular and biochemical studies to show several novel functions of MEIKIN during mouse oocyte meiotic maturation and early embryonic development. First, we show that MEIKIN is phosphorylated through PLK1-mediated phosphorylation after resumption of the first meiosis and the C-terminus was its key functional domain; then we reveal that reduced MEIKIN level is important for degradation of cyclin B1 and Securin as well as meiotic metaphase–anaphase transition; finally, we find that decreased level of MEIKIN is a prerequisite for second meiosis resumption and embryo development.

Materials and methods

Animals

ICR mice at 6–8 weeks of age were purchased from SPF (Beijing) Biotechnology Co., Ltd and raised in the SPF environment with 12 h light and 12 h dark at constant temperature (23 ± 1 °C) and humidity (60 ± 5%). All animal

experiments conformed to the animal ethics of the Institute of Zoology, Chinese Academy of Sciences.

Oocyte collection and culture

For collection of germinal vesicle (GV) oocytes, female ICR mice at 6–8 weeks of age were killed, and the ovaries were isolated and dissected in M2 culture solution supplemented with 100 μM IBMX to maintain oocytes at the GV stage. After specific treatment, oocytes were washed in fresh M2 medium and then cultured in vitro to specific stages. The MII oocytes were collected according to the following procedures (Fan et al. 2019). Female ICR mice at 6–8 weeks of age were superovulated by intraperitoneal injection (IP) with 10 U of PMSG (pregnant mare serum gonadotropin) followed by IP with 10 U of HCG (human chorionic gonadotropin). MII oocytes were collected at 13–15 h of HCG injection. Cumulus cells were disaggregated with 0.2–0.3% hyaluronidase. The MII oocytes were parthenogenetically activated by using 10 mM $SrCl_2$ in Ca^{2+}/Mg^{2+}-free CZB.

For zygote collection, female mice were immediately mated with fertile males after HCG injection following 48 h of PMSG injection. Then the zygotes were obtained from plugged female mice at 20 h of HCG injection. The zygotes were cultured in KSOM medium. All oocytes and zygotes were cultured in specific medium under liquid paraffin oil at 37 °C in a 5% CO_2 incubator.

Antibodies and inhibitors

Mouse monoclonal anti-c-Myc antibody was purchased from Sigma Chemical Company (3050 Spruce Street, Saint Louis, MO 63103, USA, m4439), mouse monoclonal anti-Myc-FITC antibody was purchased from Thermo Fisher Scientific Inc (3747 N. Meridian Road Rockford, IL 61105 USA, R953-25), rabbit polyclonal anti-Bub3 antibody (sc-28258) and mouse IgG (sc-2025) were purchased from Santa Cruz Biotechnology (10410 Finnell Street Dallas, Texas 75,220 USA). Human anti-centromere antibody (ACA) was purchased from Antibodies Incorporated (8 Station Court Station Road Cambridge CB22 5NE UK, 15-234-0001), rabbit polyclonal anti-cyclin B1 antibody was purchased from Santa Cruz Biotechnology (SC-752), rabbit monoclonal anti-beta-actin antibody was purchased from ABclonal Co., Ltd. (500W Cummings Park, Ste. 6500 Woburn, MA 01801, AC026), mouse monoclonal anti-α-tubulin antibody was purchased from Beijing Biodragon Immunotechnologies Co., Ltd. (Beijing, China, B1052). F594-conjugated goat anti-mouse IgG was purchased from Thermo Fisher Scientific Inc (3747 N. Meridian Road Rockford, IL 61105 USA, A-11005). HRP-conjugated goat anti-mouse IgG and HRP-conjugated goat anti-rabbit IgG were purchased from Zhongshan Golden Bridge Biotechnology Co. Ltd. (Beijing, China). Cy5-conjugated goat anti-human IgG and Cy5-conjugated goat anti-rabbit IgG were purchased from Jackson ImmunoResearch Laboratory (872 West Baltimore Pike West Grove, Pennsylvania 19,390 USA).

The inhibitors (nocodazole, roscovitine, AZ3146, BI6727, ZM447439, LY317615, TBB, VX702) were purchased from Selleck Biotechnology Co., Ltd (14408 W Sylvanfield Drive, Houston, TX 77014 USA).

Meikin plasmid construction and mRNA synthesis

Total RNA was extracted from 100 oocytes using Dynabeads® mRNA DIRECT™ Micro Kit (61021; Thermo Fisher Scientific) following the manufacturer's instructions, and reverse transcription was performed with All-In-One RT MasterMix (G485; Abm, 1957 Baltic Way, Unit E105 Ferndale, WA, USA). The following two nest primers were used to amplify the full-length CDS sequence of mouse *Meikin* by PCR. *Meikin*-F1: 5′-ATTACCTCGGGAAGGCAATG-3′; *Meikin*-R1: 5′-GGCAGACATTCTGCTTCTAT-GG-3′; *Meikin*-F2: 5′-GCAGGCCGGCCAATGGACAAGATATG-3′; *Meikin*-R2: 5′-GTTGGCGCGCCTTATGTTCTGCCATT-3′. *Meikin* N-terminal region primers, *Meikin*-F2 and *Meikin-N*-R1: 5′-GTTGGCGCGCCTTATTCAAGAGCTGAACTTA-G-3′. *Meikin* C-terminal region primers, *Meikin-C*-F1: 5′-GAAGGCCGGCCAAGCACTGCAGTCAG-3′ and *Meikin*-R2. The PCR products were purified, then digested using FseI and AscI (New England Biolabs, Inc. 240 County Road Ipswich, MA, USA) and cloned into the pCS2+ vector, in which the *Meikin* sequence was linked to six *Myc* tags at its N-terminus. The *Securin* plasmids and *Ccnb1* plasmids were provided by Drs. HY Fan and JY Ma, respectively.

For the synthesis of *Myc*-tagged *Meikin* mRNA, the *Meikin*-pCS2+ plasmids were linearized by KpnI and then purified. The SP6 mMESSAGE mMACHINE (Thermo Fisher Scientific Inc.) was used to produce capped mRNA. The mRNAs were then polyadenylated using a Poly(A) polymerase tailing kit (Epicentre), and purified by RNeasy clean up kit (Qiagen).

For the synthesis of *mCherry-Securin* mRNA and *GFP-Ccnb1* mRNA, the *Securin* plasmids and *Ccnb1* plasmids were linearized by KpnI and then purified. The SP6 mMESSAGE mMACHINE (Ambion) was used to produce capped mRNA. The mRNAs were then polyadenylated using a Poly(A) polymerase tailing kit (Epicentre), and then purified by RNeasy clean up kit (Qiagen). The concentration was detected with a Beckman DU 530 Analyzer, and diluted to 0.1 μg/μl for localization and 1.0 μg/μl for overexpression.

Microinjection of mRNA and siRNA

Microinjections were performed using a Narishige microinjector for GV oocytes and were performed using piezo microinjector of Primetech for MII oocytes and zygotes. All microinjections were completed within 30 min. Each oocyte was microinjected with 7–10 pl mRNA or siRNA.

For Myc-Meikin expression, *Myc–Meikin* mRNA solution was injected into cytoplasm of GV oocytes. For protein expression, oocytes were arrested at the GV stage in M2 medium supplemented with 100 μM IBMX for 12 h. The same dose RNase-free water was injected as control.

For knockdown experiments, small interfering RNAs (siRNAs) were microinjected into the cytoplasm to deplete endogenous protein. The subsequent siRNAs were used at 20–40 mM. After siRNA injection, oocytes were arrested at the GV stage in M2 medium supplemented with 100 μM IBMX for 24 h for the depletion of endogenous protein. All siRNAs were listed as follows. *Mad2* siRNA: 5′-GGA CUCACCUUGCUUACAAtt-3′; *Securin* siRNA: 5′-GAU GAUGCCUACCCAGAAAtt-3′; *PKCβ* siRNA-1: 5′-GCA GGGAUUCCAGUGUCAAtt-3′ and *PKCβ* siRNA-2: 5′-GCUGCUGUAUGGACUUA UUtt-3′; Negative control siRNA: 5′-UUCUCCGAACGUGUCACGUtt-3′.

Western blotting

Oocytes at the appropriate stages of meiotic maturation were collected and transferred to 5 μl 2 × SDS sample buffer and boiled for 5 min. The samples were separated by SDS-PAGE and then transferred to PVDF membranes. After transfer, the membranes were washed twice for 10 min each in TBST buffer (50 mM Tris, 150 mM NaCl, 0.1% Tween 20, pH 7.4) and then blocked in TBST buffer containing 5% skimmed milk, for 1.5–2 h at room temperature, followed by incubation overnight at 4 °C primary antibodies with appropriate concentrations according to the manufacturer's instructions. After three washes for 10 min each in TBST buffer, the membranes were incubated with 1:2000 corresponding HRP-conjugated secondary antibodies, for 1–2 h at 37 °C. Finally, the membranes were washed three times for 10 min each in TBST and processed using the enhanced chemiLuminescence detection system (Bio-Rad, CA).

Lambda protein phosphatase treatment

Oocytes were collected and transferred to 3 μl RIPA lysis solution (R0010; Solarbio) on ice for 10 min, with PMSF to prevent total protein degradation. Then 2 μl Lambda Protein Phosphatase (P0753; NEB) was added to the lysis solution, with 1 × PMP buffer (50 mM HEPES, 100 mM NaCl, 2 mM DTT, and 0.01% Brij 35) and 1 mM $MnCl_2$, at 30 °C for 30 min. After treatment with Lambda Protein Phosphatase, 5 × SDS sample buffer was added and the sample was boiled for 5 min for western blotting.

Immunofluorescence and chromosome spread

Oocytes were fixed in 4% paraformaldehyde in PBS buffer with 0.5% Triton X-100 for 30 min and then blocked in 1% BSA-supplemented PBS for 1.5–2 h at room temperature. Then oocytes were incubated with primary antibody at appropriate concentrations overnight at 4 °C. After three washes for 5 min each in washing buffer (0.1% Tween 20 and 0.01% Triton X-100 in PBS), oocytes were incubated with corresponding secondary antibody for 1–2 h at room temperature, then washed three times. DNA was stained with DAPI for 15 min. Oocytes were mounted on glass slides with 3–5 μl DABCO to prevent fluorescence quenching for immunofluorescence microscopy. Photos were taken with a confocal laser-scanning microscope, LD Plan-Neofluar: ×20 (0.8 NA), ×40 (0.95 NA), ×60 oil (1.4 NA), (Zeiss LSM 780, Germany). DAPI: laser 405 nM/30mW, filter 420–480 nM. Fitc: AXlaser 488 nM/25mW, filter 500–550 nM. F594: HeNelaser 561 nM/20mW, filter 590–630 nM. CY5: HeNelaser 633 nM/5 mW, filter 640 nM.

Chromosome spreads were performed as described previously (Hodges and Hunt 2002). Briefly, the oocytes were exposed to acid Tyrode's solution (Sigma) for 3 min at room temperature to remove the zona pellucida. After a brief recovery in M2 medium, the oocytes were transferred onto glass slides and fixed in a solution of 1% paraformaldehyde in distilled H_2O (pH 9.2) containing 0.15% Triton X-100 and 3 mM dithiothreitol. The slides were allowed to dry slowly in a humid chamber for several hours, and then blocked with 1% BSA in PBS for 1.5–2 h at room temperature. The oocytes were incubated with primary antibodies at appropriate concentrations overnight at 4 °C according to the manufacturer's instructions. Mouse IgG replaced primary antibody in the control experiment for immunofluorescence. After brief washes with washing buffer, the slides were then incubated with the corresponding secondary antibodies for 1–2 h at room temperature. DNA on the slides was stained with DAPI and slides were mounted with 3–5 μl DABCO to prevent fluorescence quenching for observation by immunofluorescence microscopy.

Time-lapse live imaging

Cyclin B1 or Securin and chromosome dynamics were filmed on a PerkinElmer precisely Ultra VIEW VOX Confocal Imaging System, equipped with a CO_2 incubator chamber (5% CO_2 at 37 °C) in M2 medium covered with mineral oil. The digital time-lapse images (26 z slices with 2 μm spacing) were acquired using a ×20 0.75 objective lens, and Volocity 6.0 software was used for image acquisition.

Oocytes were injected with *GFP-Ccnb1* or *mCherry-Securin* mRNA. Injected oocytes were incubated in M2 medium supplemented with 2.5 mM milrinone for 2–3 h to express the exogenous proteins and DNA was stained with Hoechst 33342 for 30 min. Then, the oocytes were released into M2 medium and prepared for time-lapse imaging. To image oocyte maturation with GFP-cyclin B1 and mCherry-Securin, images were taken every 20 min for 17 h. Exposure time was set ranging between 300 and 800 ms depending on the GFP or mCherry and Hoechst 33342 fluorescence levels. Confocal images of cyclin B1 or Securin and chromosomes in live oocytes were acquired with a ×20 oil objective on a spinning disk confocal microscope (PerkinElmer).

Real-time quantitative PCR analysis

Oocyte RNA was extracted with Dynabeads® mRNA DIRECT™ Micro Kit following the manufacturer's instructions. Reverse transcription was performed with All-In-One RT MasterMix. RT-qPCR was performed with FastStart Universal SYBR Green Master mix (CW0957S; CWbiotech) and gene-specific primers using a Real-Time PCR machine (Applied Biosystems). The steps consisted of 95 °C for 15 s, 40 cycles of 95 °C for 5 s and 60 °C for 30 s. Relative gene expression was calculated by the 2DDCt method. PCR primers used in the present study were listed as follows. *Meikin*-rt-F1: 5′-CTATACCCGCAAGAAGAGGGC-3′; *Meikin*-rt-R1: 5′-TGCTACCTGTGAGTCTGCTC-3′; *Mad2l1*-F1: 5′-GTGGCCGAGTTTTTCTCATTTG-3′; *Mad2l1*-R1: 5′-AGGTGAGTCCATATTTCTGCACT-3′; *Securin*-F1: 5′-AACCCCTCCAACCAAAACAG-3′; *Securin*-R1: 5′-TCTGGGTAGGCATCATCAGGA-3′; *Gapdh*-F1: 5′-AGGTCGGTGTGAACGGATTTG-3′; *Gapdh*-R1: 5′-TGTAGACCATGTAGTTGAGGTCA-3′.

Statistical analysis

All experiments were repeated at least three times. All percentages are expressed as means ± standard error (SEM), and the numbers of oocytes observed (*n*) are given in parentheses. Data were analyzed by independent-sample *t* tests and one-way analysis of variance (ANOVA), followed by Tukey's multiple comparisons test. $P < 0.05$ was considered statistically significant.

Results

Expression and localization of MEIKIN during mouse oocyte meiotic maturation

To examine the expression level of meikin during mouse oocyte meiotic maturation and early embryonic development, mouse oocytes were collected at 0 h, 8 h, 12 h, corresponding to germinal vesicle (GV), MI, and MII stages of meiotic maturation, and zygotes were also collected directly for real-time quantitative PCR analysis. The results showed that the mRNA level of *Meikin* was the highest at the GV and MI stages and then slightly decreased at the MII stage at a rate of 26.8% compared to the GV stage. However, at the zygote stage the mRNA level of *Meikin* was significantly decreased at a rate of 75.6% compared to the GV stage (Fig. 1a).

Because of the lack of workable antibodies for immunofluorescence staining to determine the subcellular localization of MEIKIN, a low concentration of exogenous *Myc-Meikin* mRNA in nuclease-free water was injected into mouse oocytes at the GV stage; for the control, only nuclease-free water was injected at the equal dose. The oocytes were then cultured to different stages of meiotic maturation. Anti-Myc antibody was used to detect the localization of Myc-MEIKIN for immunofluorescence microscopy. As shown in Figs. 1b and S1, Myc-MEIKIN was evenly distributed in the cytoplasm and nucleus of the GV oocyte except for the nucleolus. After the germinal vesicle breakdown (GVBD) to MI stages, chromosomes arranged on the equatorial plate and Myc-MEIKIN was strongly accumulated around centromeres of chromosomes. At the MII stage, following homologous chromosome segregation, the signal of Myc-MEIKIN at centromeres was faint. And there was no signal of Myc-MEIKIN in the four stages of meiotic maturation in the negative control (Fig. S1).

In addition, we employed the method of chromosome spreading to further define the MEIKIN localization on centromeres. As shown in Fig. 1c, at the MI stage Myc-MEIKIN was clearly localized on centromeres of chromosomes and colocalized with ACA. At the MII stage, MEIKIN was colocalized with ACA at chromosomes, but the signals were faint. Thus, we conclude that MEIKIN may play an important role in regulating meiotic progression.

Exogenous MEIKIN expression causes misaligned chromosomes and reduced polar body emission

The MEIKIN expression pattern mentioned above indicates that dynamic MEIKIN change may play an important role in regulating meiotic progression. A previous study has shown that MEIKIN can regulate the mono-orientation of sister kinetochores by way of gene knockout (Kim et al. 2015). To further investigate the function of MEIKIN in meiosis, exogenous MEIKIN was expressed in mouse oocytes. The GV oocytes were injected with *Myc-Meikin* mRNA or nuclease-free water as the control. The injected oocytes were incubated for 12 h in M2 medium containing 200 μM IBMX for the expression of Myc-MEIKIN protein. Then the oocytes were released from IBMX and cultured in M2

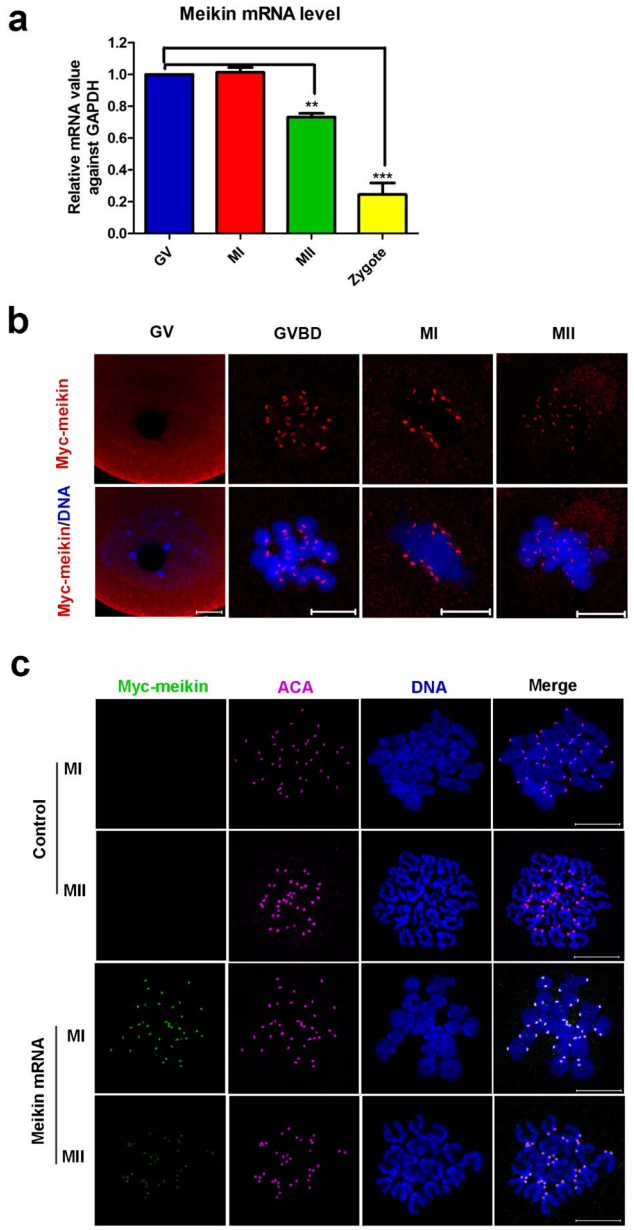

Fig. 1 Expression and localization of MEIKIN during mouse oocyte meiotic maturation. **a** Expression level of *Meikin* mRNA as revealed by RT-PCR. A total of 100 GV, MI, and MII oocytes or zygotes were collected for RT-PCR. *GAPDH* was used as the internal reference gene and the mRNA expression level at the GV stage was normalized to 1. Data are expressed as mean ± SEM of at least three repeats, $P < 0.0001$. **b** Immunofluorescence staining to determine the subcellular localization of MEIKIN. Oocytes at the GV stage were injected with *Myc-Meikin* mRNA (0.1 μg/μl) or an equal dose of RNase-free water and inhibited for 2 h with IBMX, and cultured to different stages. Myc antibody was used to detect the localization of Myc-MEIKIN (red) in the oocytes. DNA was labeled with DAPI (blue). Scale bars: 10 μm. **c** The colocalization of MEIKIN and ACA by chromosome spreading. GV stage oocytes were injected with *Myc-Meikin* mRNA (0.1 μg/μl) or an equal dose of RNase-free water, and cultured to MI and MII stages. Then chromosomes were spread and stained with Myc antibody (green), ACA (anti-centromere antibody, purple), and DNA (DAPI, blue). Scale bars: 10 μm

medium to resume meiosis. Western blotting was conducted to confirm the expression of Myc-MEIKIN after exogenous mRNA injection. As presented in Fig. 2a, in the exogenous MEIKIN expression group, a clear Myc-MEIKIN blot was observed at approximately 70 kDa; however, in the control group no specific blot was detected.

Then we observed the oocyte maturation phenotypes and found that exogenous MEIKIN expression had little effect on oocyte meiotic resumption. The GVBD rate of the exogenous MEIKIN expression group was 75.4 ± 5.6% and that of the control group was 73.8 ± 3.8%. However, exogenous MEIKIN expression significantly prevented first polar body emission (PBE). The rate of PBE in the exogenous MEIKIN expression group (11.9 ± 5.2%) was remarkably lower than that in the control group (90.9 ± 3.5%), as shown in Fig. 2b.

To understand how exogenous MEIKIN expression inhibits PBE, the injected oocytes were cultured for 14 h and collected for immunofluorescence and chromosome spreading to observe the spindle and chromosome morphology. The result of immunofluorescence (Fig. 2c) showed that after culture of 14 h, the homologous chromosomes had segregated in the control group, while in the overexpression group the homologous chromosomes were still attached. The same result was also obtained through chromosome spreading (Fig. 2c).

To further reveal the reason for the suppression of PBE caused by exogenous MEIKIN expression, we collected oocytes at 8 h of in vitro culture and examined the MI spindle morphology and chromosome distribution. We observed that after 8 h of culture, in the control group most oocytes had entered the MI stage along with homologous chromosomes orderly aligned at the equatorial plate, but in the exogenous MEIKIN expression group the oocytes showed misaligned chromosomes (Fig. 2d). The rate of abnormal spindles (Fig. 2e) in the exogenous MEIKIN expression group (12.8 ± 3.9%) was higher than that in the control group (3.4 ± 2.3%). The rate of misaligned chromosomes (Fig. 2e) in the exogenous MEIKIN expression group (67 ± 5.2%) was significantly higher than that in the control group (29.3 ± 3.1%). The metaphase plate width in the exogenous MEIKIN expression group (20.2 ± 1.0 μM) was significantly higher than that in the control group (15.4 ± 0.6 μM) (Fig. 2f). These results indicate that exogenous MEIKIN expression causes misaligned chromosomes and thus reduces PBE.

Exogenous MEIKIN expression inhibits MII exit and early embryonic development

Because MEIKIN is a maternal factor with low expression level in the MII stage and zygote, we wanted to know whether MEIKIN decrease is required for subsequent development. To test this, MII oocytes were injected with

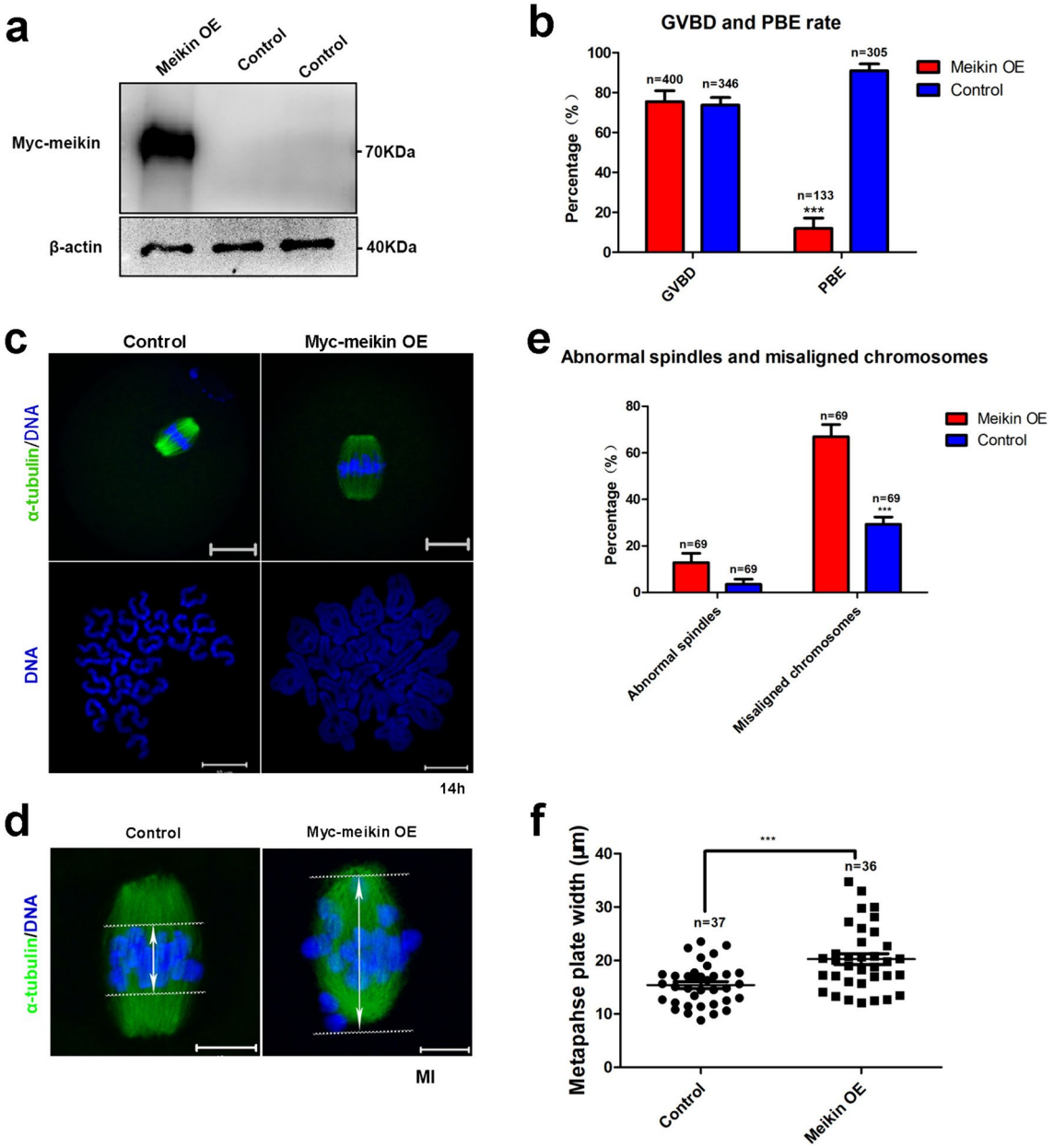

Fig. 2 Exogenous MEIKIN overexpression causes misaligned chromosomes and reduces PBE. **a** Expression of exogenous *Myc-Meikin* mRNA in GV oocytes. The high concentration (1 μg/μl) *Myc-Meikin* mRNA or the equal dose RNase-free water was injected into GV stage oocytes and the oocytes were inhibited for 12 h with IBMX. A total of 100 GV oocytes were collected in each lane for western blotting and the level of β-actin was used as the internal control. **b** The rates of GVBD and PBE. After overexpressing MEIKIN, the oocytes were cultured for 14 h. The rates of GVBD and PBE were calculated respectively. **c** The morphology of spindles and chromosomes at the MII stage. After overexpressing meikin, the oocytes were cultured for 14 h. The oocytes were collected for immunofluorescence staining to detect the morphology of the spindle (α-tubulin, green) or for chromosome spreading to detect the morphology of chromosomes (DAPI, blue). Scale bars: 10 μm. **d** The morphology of spindles at the MI stage. After overexpressing MEIKIN, the oocytes were cultured for 8 h. The oocytes were collected for immunofluorescence staining to detect the morphology of the spindle (α-tubulin, green) and chromosomes (DAPI, blue). Scale bars: 10 μm. **e** The percentage of abnormal spindles and misaligned chromosomes at the MI stage in overexpression and control oocytes. **f** The width of chromosome arrangement range (metaphase plate width) in oocytes of overexpression and control group. Data are presented as mean ± SEM of at least three repeats. n stands for the total number of oocytes. ***$P < 0.001$

Myc-Meikin mRNA or nuclease-free water (control) and cultured for 2 h to allow protein expression; then the oocytes were artificially activated for 3 h with 10 mM $SrCl_2$ in Ca^{2+}/Mg^{2+}-free CZB. The results of immunofluorescence (Fig. 3a, b) showed that most of the oocytes in the control group (94.4 ± 2.8%) had extruded the second polar body and

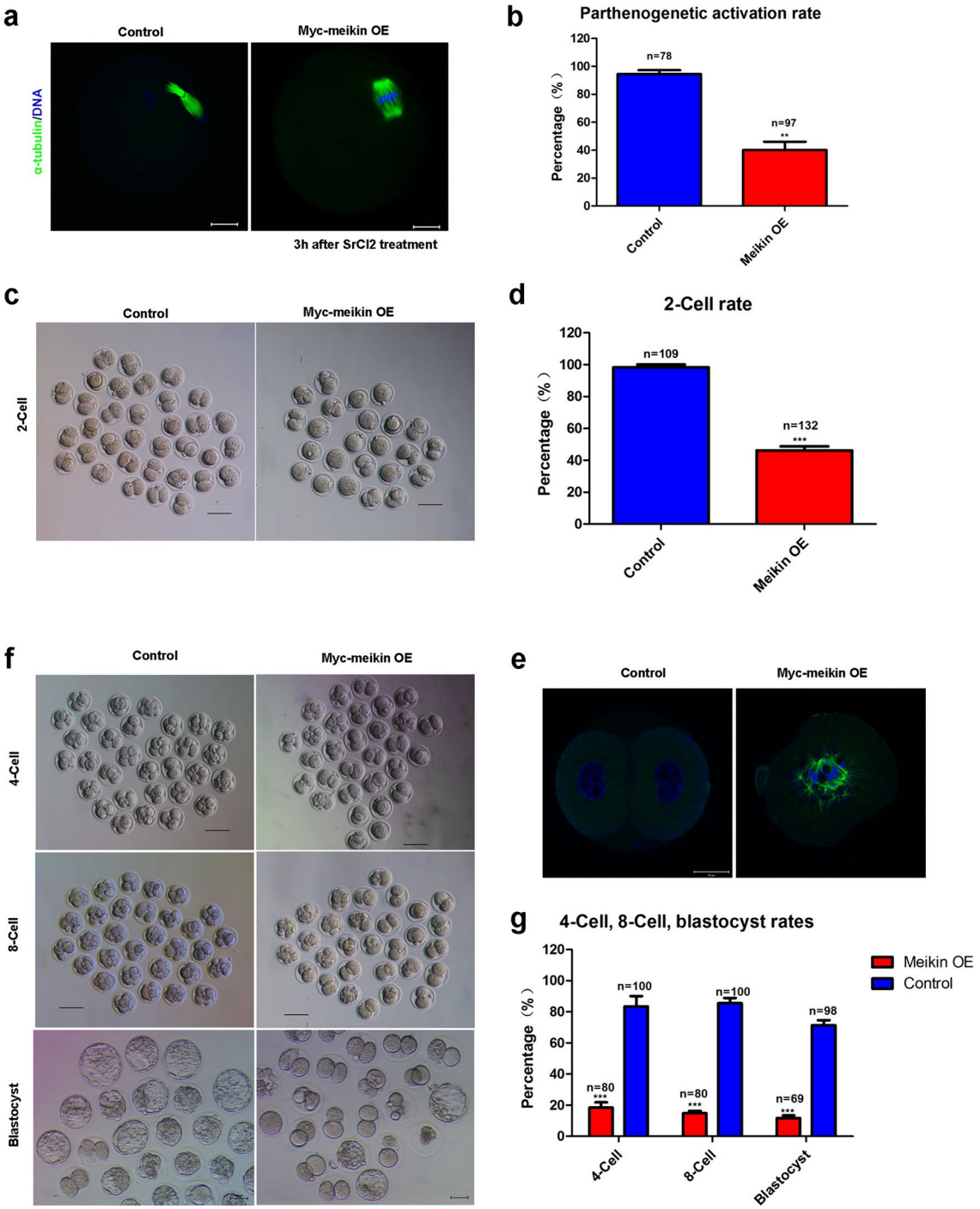

Fig. 3 Exogenous MEIKIN overexpression inhibits MII exit and early embryonic development. **a** The morphology of spindles and chromosomes at MII stage after 3 h parthenogenetic activation. The high concentration (1 μg/μl) *Myc-Meikin* mRNA or the equal dose RNase-free water was injected into MII stage oocytes. After 2 h of culture, the oocytes were activated with $SrCl_2$ for 3 h and collected for immunofluorescence staining to detect the morphology of the spindles (α-tubulin, green) and chromosomes (DAPI, blue). Scale bars: 20 μm. **b** The rate of parthenogenetic activation in overexpression and control oocytes. **c** The 2-cell rate in overexpression and control embryos. Zygotes were injected with high concentration (1 μg/μl) *Myc-Meikin* mRNA or the equal dose RNase-free water and cultured in vitro for 24 h to observe the development of embryos. Scale bars: 100 μm. **d** Then the rate of 2-cell stages was calculated. **e** The embryos were collected for immunofluorescence staining to observe the morphology of the spindles (α-tubulin, green) and chromosomes (DAPI, blue). **f**, **g** The rates of 4-cell, 8-cell, and blastocyst in overexpression and control embryos. After overexpressing MEIKIN, the zygotes were cultured to blastocysts. The rates of 4-cell, 8-cell, and blastocysts were calculated, respectively. The data are expressed as mean ± SEM of at least three repeats. n stands for the total number of oocytes. $^{**}P < 0.01$; $^{***}P < 0.001$

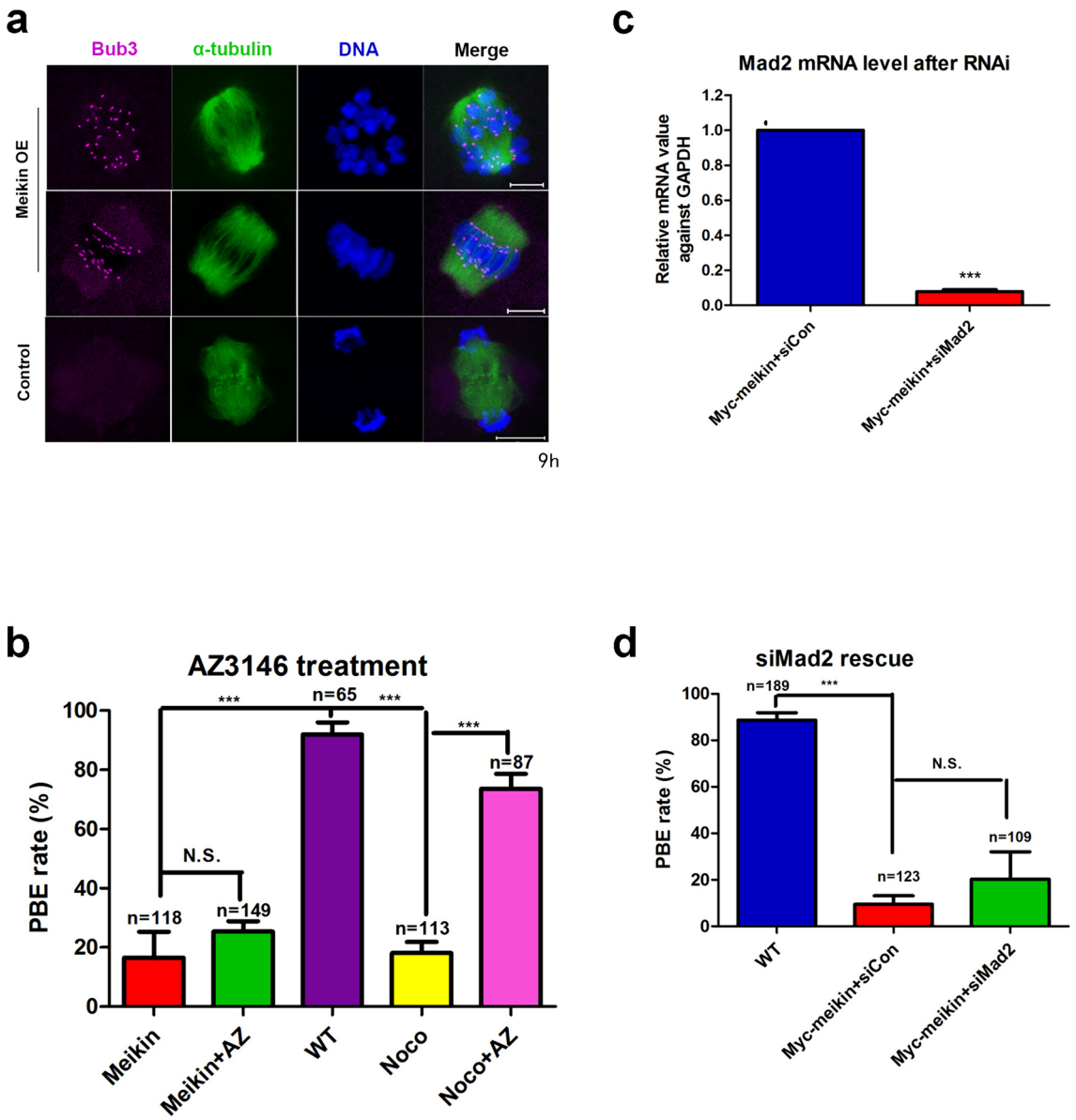

Fig. 4 Exogenous MEIKIN expression activates the SAC, but inhibition of the SAC does not rescue MI arrest caused by MEIKIN overexpression. **a** The detection of Bub3 at 9 h of culture. After overexpressing MEIKIN, the oocytes were cultured for 9 h and collected for immunofluorescence staining to detect Bub3 (purple), the spindle (α-tubulin, green), and chromosomes (DAPI, blue). Scale bars: 10 μm. **b** AZ3146 treatment did not rescue MI arrest caused by MEIKIN overexpression. After overexpressing MEIKIN, the oocytes were cultured in medium containing 5 μM AZ3146 or an equal dose DMSO for 14 h. The WT oocytes at GV stages were cultured in medium containing either nocodazole or nocodazole + AZ3146 to detect the effect of AZ3146 on inhibiting SAC, $P < 0.0001$. **c** Levels of *Mad2* mRNA after RNAi. *Myc-Meikin* mRNA (μg/μl) plus *Mad2* siRNA (siMad2, 40 μM) or the same dose control siRNA (*siCon*) was injected into the GV oocytes, and the oocytes were inhibited for 24 h with IBMX. Oocytes were collected to detect the levels of *Mad2* mRNA by RT-PCR, with *GAPDH* as the internal reference gene. Then the oocytes were released and cultured for 14 h. The rate of PBE in each group was calculated, $P = 0.0005$. **d** The data are expressed as mean ± SEM for at least three repeats. N.S. indicates no significant difference. $^{**}P < 0.01$; $^{***}P < 0.001$

went through anaphase II, while exogenous MEIKIN expression caused failure of the second meiosis resumption, and 59.9% oocytes were still arrested at the MII stage.

To examine the role of exogenous MEIKIN expression in embryonic development, the zygotes were injected with *Myc-Meikin* mRNA or nuclease-free water (control). The results (Fig. 3c, d) showed that the 2-cell rate in the exogenous MEIKIN expression group (46.3 ± 2.5%) was dramatically lower than that in the control group (98.3 ± 1.7%). Immunofluorescence detection (Fig. 3e) confirmed that

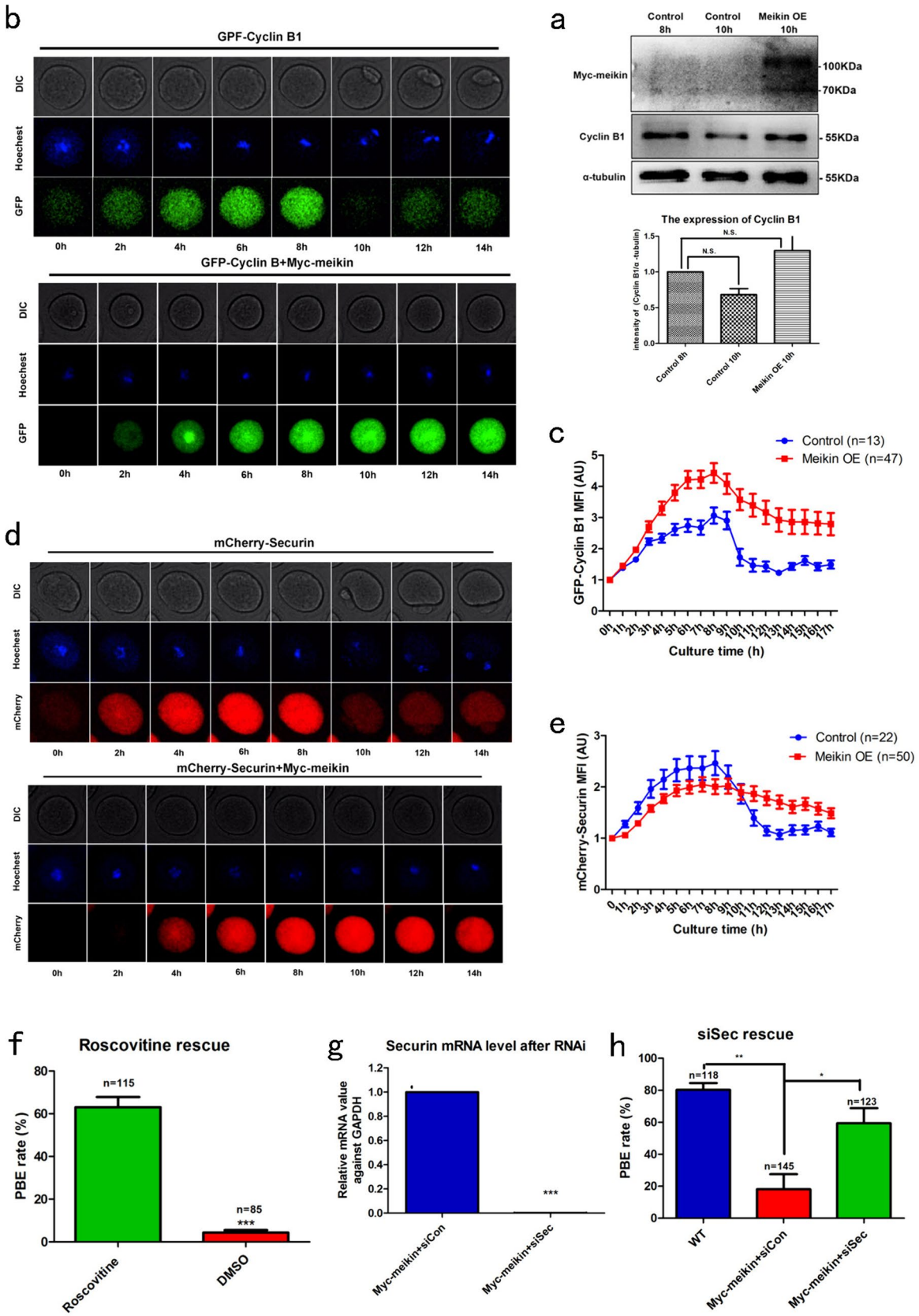
b
GPF-Cyclin B1
DIC
Hoechest
GFP
0h 2h 4h 6h 8h 10h 12h 14h
GFP-Cyclin B+Myc-meikin
a
Control 8h
Control 10h
Meikin OE 10h
Myc-meikin
Cyclin B1
α-tubulin
100KDa
70KDa
55KDa
55KDa
The expression of Cyclin B1
Intensity of (Cyclin B1/α -tubulin)
N.S.
N.S.
Control 8h
Control 10h
Meikin OE 10h
c
Control (n=13)
Meikin OE (n=47)
GFP-Cyclin B1 MFI (AU)
Culture time (h)
d
mCherry-Securin
mCherry
mCherry-Securin+Myc-meikin
e
Control (n=22)
Meikin OE (n=50)
mCherry-Securin MFI (AU)
Culture time (h)
f
Roscovitine rescue
PBE rate (%)
n=115
n=85
***
Roscovitine
DMSO
g
Securin mRNA level after RNAi
Relative mRNA value against GAPDH
*
***
Myc-meikin+siCon
Myc-meikin+siSec
h
siSec rescue
PBE rate (%)
n=118
n=145
n=123
**
*
WT
Myc-meikin+siCon
Myc-meikin+siSec

◂**Fig. 5** Exogenous MEIKIN expression inhibits the degradation of cyclin B1 and Securin, which can be rescued by inhibition of CDK or Securin. **a** The expression level of cyclin B1. After overexpressing MEIKIN, the oocytes were cultured for 8 h or 10 h and collected for western blotting to detect the expression level of cyclin B1. The intensity of cyclin B1/α-tubulin was accessed by grayscale analysis. A total of 50 oocytes were collected in each lane and the level of α-tubulin was used as the internal control, $P=0.45$. **b** The dynamic change of cyclin B1expression level during oocyte meiotic maturation. The GV oocytes were injected with *GFP-Ccnb1* mRNA (0.02 μg/μl) plus *Myc-Meikin* mRNA (1 μg/μl) or the same dose of RNase-free water, inhibited for 2 h with IBMX, and then cultured to observe the dynamic change of GFP-cyclin B1 expression by live-cell imaging. **c** The fluorescence intensity of GFP-cyclin B1 was measured every 20 min for 17 h to obtain the fluorescence intensity curve. **d** The dynamic change of Securin expression level during oocyte meiotic maturation. The GV oocytes were injected with *mCherry-Securin* mRNA (0.1 μg/μl) plus *Myc-Meikin* mRNA (1 μg/μl) or the same dose of RNase-free water, inhibited for 2 h with IBMX, and then cultured to observe the dynamic change of mCherry-Securin expression by live-cell imaging. **e** The fluorescence intensity of mCherry-Securin was measured every 20 min for 17 h to obtain the fluorescence intensity curve. **f** The PBE rescue by roscovitine. The oocytes with overexpressed MEIKIN were cultured for 14 h; then oocytes blocked at the MI stage were collected and transferred to the medium with 200 μM roscovitine or the same dose of DMSO, and cultured for another 6 h. The PBE rate was calculated. **g** The mRNA level of *Securin* after RNAi. *Myc-Meikin* mRNA (1 μg/μl) plus *Securin* siRNA (*siSec*, 40 μM) or the same dose control *siRNA* (*siCon*) was injected into the GV oocytes, and the oocytes were inhibited for 24 h with IBMX. Oocytes were then collected to detect the level of *Securin* mRNA by RT-PCR, with *GAPDH* as the internal reference gene. Then the oocytes were released and cultured for 14 h. **h** The rate of PBE in each group was calculated, $P=0.0045$. The data are expressed as mean ± SEM of at least three repeats. n is the total number of observed oocytes. $^{*}P<0.05$; $^{**}P<0.01$; $^{***}P<0.001$

zygotes in the exogenous MEIKIN expression group halted the first division stage after 24 h of in vitro culture, while zygotes in the control group had entered the 2-cell stage. We also found that the 4-cell rate (18.4 ± 3.7%), 8-cell rate (14.9 ± 1.5%), and blastocyst rate (11.7 ± 1.7%) in the exogenous meikin expression group (83.5 ± 6.7%, 85.5 ± 3.4%, 71.5 ± 3.2%) were all dramatically lower than in the control group (Fig. 3f, g). The results indicate that exogenous MEIKIN expression inhibits MII exit and retards embryonic development.

Exogenous MEIKIN expression activates the SAC, but inhibition of the SAC does not rescue MI arrest

Because exogenous MEIKIN overexpression caused chromosome misalignment and MI arrest, we examined whether this was achieved by activating the SAC. To confirm this, the overexpressed oocytes were cultured for 9 h and collected for immunofluorescence to detect the localization of Bub3, one of the primary components of SAC. The result showed that specific signal for Bub3 was detected in the exogenous MEIKIN expression group after 9 h of culture (Fig. 4a), and the oocytes were arrested at the Pro-MI/MI stage. In contrast, most of the control oocytes had entered anaphase and showed no signal of Bub3. The result verified that SAC was activated in the exogenous MEIKIN expression oocytes.

To confirm whether the activation of SAC was the only reason to cause MI arrest by exogenous MEIKIN expression, we artificially inhibited SAC. We found that the MPS1 (one of the primary components of SAC) inhibitor AZ3146 could rescue the MI arrest by nocodazole (spindle assembly inhibitor) treatment in WT oocytes (73.6 ± 5.0% vs 18.1 ± 3.7%). However, in exogenous MEIKIN expression oocytes, AZ3146 treatment only slightly increased the PBE rate and the difference was not obvious between AZ3146 treatment and no-AZ3146 treatment oocytes (25.4 ± 3.5% vs 16.6 ± 8.7%) (Fig. 4b). The result indicated that AZ3146 treatment did not rescue MI arrest by exogenous MEIKIN expression. Secondly, we injected Mad2 (one of the primary components of SAC) siRNA to inhibit the SAC. The real-time PCR result showed successful depletion of Mad2 (7.8 ± 1.1%) (Fig. 4c). We found that depletion of Mad2 only slightly increased the PBE rate in exogenous MEIKIN expression oocytes and the PBE rate displayed no obvious difference between *siMad2* and *siCon* (20.3 ± 11.8% vs 9.5 ± 3.6%) (Fig. 4d) groups. Thus, exogenous MEIKIN expression activated the SAC, but inhibition of the SAC did not rescue MI arrest.

Exogenous MEIKIN expression inhibits the degradation of cyclin B1 and Securin, which was rescued by CDK inhibition or Securin deletion

The degradation of cyclin B1 and Securin is a prerequisite for the metaphase–anaphase transition and chromosome segregation (Clute and Pines 1999; Peters 2006); thus, we asked whether exogenous MEIKIN expression inhibited the degradation of cyclin B1 and Securin, and further caused the MI arrest. We respectively collected the control oocytes at MI (8 h) and anaphase-telophase I (10 h) stages, and oocytes with exogenous MEIKIN expression at 10 h of culture. The western blotting showed that in the control group the expression level of cyclin B1 was relatively high at 8 h of culture and became reduced at 10 h of culture, but in the exogenous meikin expression group the expression level of cyclin B1 was still high at 10 h of culture (Fig. 5a). Then we employed live cell imaging to reveal the dynamic changes of the expression level of cyclin B1 and Securin. The oocytes in the control group and MEIKIN overexpression group were respectively injected with *GFP-Ccnb1* or *mCherry-Securin* mRNA for live cell imaging. The live cell imaging showed that before the MI stage (0 h–8 h), the signals of both GFP-cyclin B1 and mCherry-Securin increased gradually and reached the highest level at the MI stage (8 h) in the

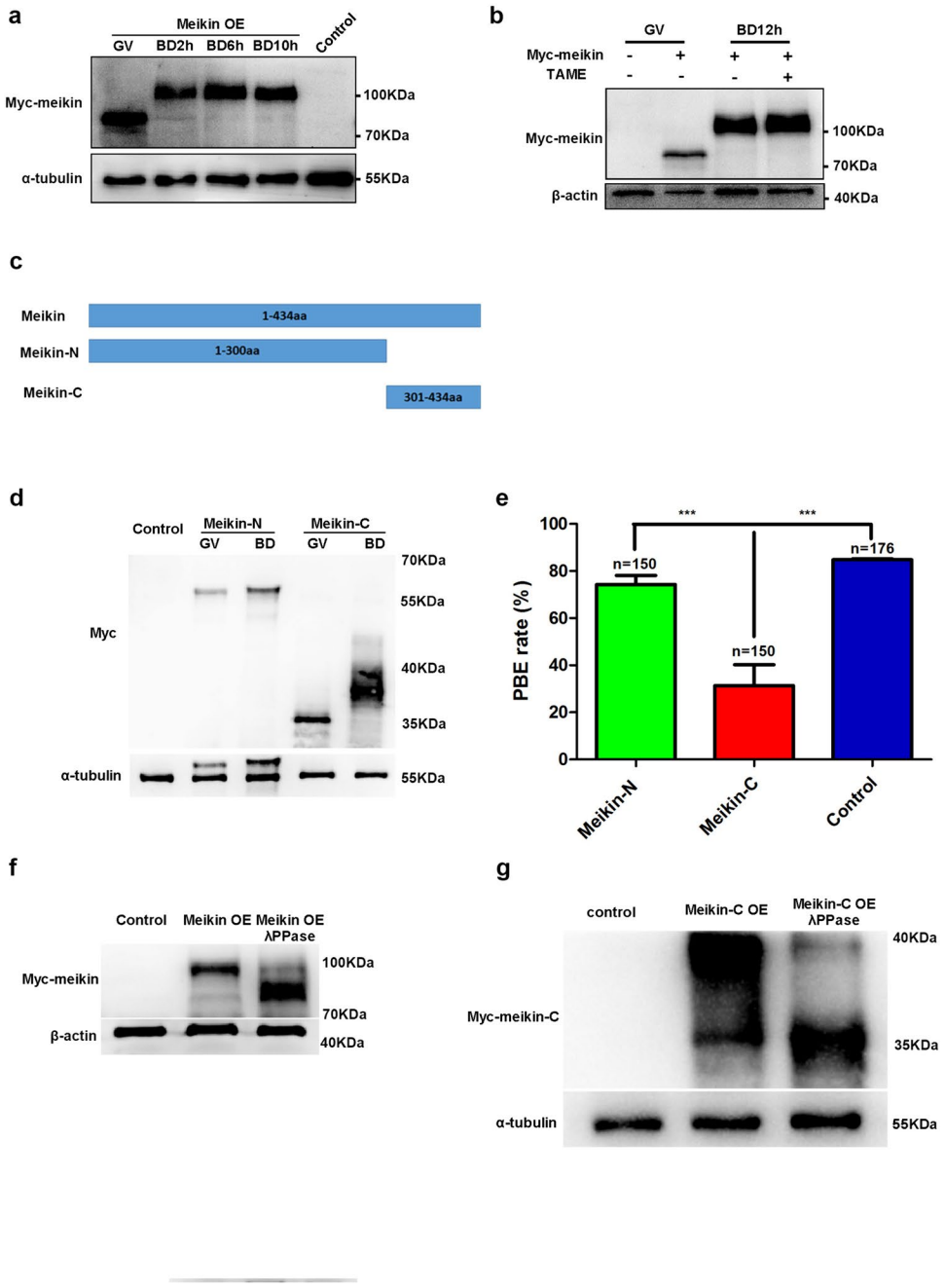

control group and exogenous MEIKIN expression group. At the metaphase–anaphase transition, the signals of GFP-cyclin B1 and mCherry-Securin declined sharply in the control group. The signals of GFP-cyclin B1 and mCherry-Securin in the MEIKIN overexpression group also declined, but the degree of decline was significantly lower than in the control group (Fig. 5b–e).

Next, we examined whether inhibition of CDK or deletion of Securin could rescue the MI arrest by exogenously expressed meikin. We used the CDK-specific inhibitor roscovitine to suppress the CDK activity. The results showed that the PBE rate in exogenous MEIKIN expression oocytes increased dramatically after roscovitine treatment (63.1 ± 4.8%) compared with DMSO treatment (control, 4.3 ± 1.1%, Fig. 5f). Next, we injected *Securin* siRNA to deplete Securin. The real-time PCR analysis (Fig. 5g) showed that the expression level of Securin was clearly reduced after injection of *siSec*. The PBE rate in the exogenous meikin expression oocytes increased significantly with injection of *siSec* (59.3 ± 9.6%) compared with that with *siCon* (18.1 ± 9.4%) in the MEIKIN overexpression oocytes (Fig. 5h). These results indicate that inhibition of cyclin B1

◂**Fig. 6** The key functional domain of MEIKIN with phosphorylation. **a** The expression changes of Myc-MEIKIN at different stages. The oocytes with overexpressed MEIKIN were cultured and collected at different stages, 0 h, 2 h, 6 h, 10 h. A total of 50 oocytes were used in each lane for western blotting, and the level of α-tubulin was used as an internal control. **b** The expression changes of Myc-MEIKIN with TAME treatment. The oocytes with overexpressed MEIKIN were cultured in a medium containing 200 μM TAME or the same dose of DMSO for 14 h. A total of 50 oocytes were used in each lane for western blotting, and the level of β-actin was used as an internal control. **c** The schematic diagram of MEIKIN-N and MEIKIN-C. MEIKIN protein (434 aa) was divided into the N-terminal (1–300 aa) and the C-terminal (301–434 aa). **d** The expression changes of Myc-MEIKIN-N and Myc-MEIKIN-C. The high concentration (1 μg/μl) *Myc-Meikin-N* or *Myc-Meikin-C* mRNA and the equal dose RNase-free water as the control were injected in GV stage oocytes and the oocytes were inhibited for 12 h with IBMX. Then the oocytes were cultured for 14 h. A total of 50 oocytes were collected in each lane for western blotting and the level of α-tubulin was used as the internal control. **e** The PBE rates of oocytes with overexpressed MEIKIN-N and MEIKIN-C. After overexpression and 14 h of culture, the PBE rate of oocytes in each group was calculated. The data are expressed as mean ± SEM for at least three repeats, $P < 0.0001$. **f** The expression changes of Myc-MEIKIN after GVBD with λPPase treatment. After MEIKIN overexpression and 14 h of culture, 50 oocytes were collected in each group for western blotting and the level of β-actin was used as the internal control. **g** The expression changes of Myc-MEIKIN-C after GVBD with λPPase treatment. After MEIKIN-C overexpression and 14 h of culture, 50 oocytes were collected in each group for western blotting and the level of α-tubulin was used as the internal control

or Securin can rescue the MI arrest caused by exogenous MEIKIN expression.

The C-terminal region of MEIKIN undergoes phosphorylation after GVBD

We observed that the molecular weight of Myc-MEIKIN changed at different stages of oocyte maturation. At the GV stage, the molecular weight of Myc-MEIKIN was approximately 70 kDa as predicted (Fig. 2a); however, at 10 h of culture, the molecular weight of Myc-MEIKIN changed to approximately 100 kDa (Fig. 5a). To study the detailed change in time of the molecular weight of Myc-MEIKIN, we collected MEIKIN overexpression oocytes at different stages for western blotting. The result showed that the molecular weight of Myc-MEIKIN had changed after GVBD (Fig. 6a). The result indicates that MEIKIN may undergo an unknown post-translational modification.

Because exogenous MEIKIN expression inhibited the ubiquitination and degradation of cyclin B1 and Securin, and the molecular weight of Myc-MEIKIN increased, we speculated that meikin was also the substrate of APC/C and underwent ubiquitination. To validate the speculation, we used TAME, an inhibitor of APC/C, to treat the oocytes. The result showed that MEIKIN still underwent the modification after TAME treatment at 12 h of culture (Fig. 6b). Thus, MEIKIN was not the substrate of APC/C.

To explore the domain of post-translational modification of MEIKIN protein, we divided MEIKIN protein (total 434 aa—amino acid) into the N-terminus (1–300 aa) and the C-terminus (301–434 aa) and constructed respectively the overexpression plasmids of *Myc-Meikin-N* and *Myc-Meikin-C* (Fig. 6c). Then we injected respectively the mRNA of *Myc-Meikin-N* and *Myc-Meikin-C* into the oocytes. We found that the molecular weight of Myc-MEIKIN -N did not change after GVBD; however, the molecular weight of Myc-MEIKIN-C increased after GVBD (Fig. 6d). The result indicates that the C-terminus of MEIKIN is the domain of post-translational modification. MEIKIN-C overexpression significantly reduced PBE (31.4 ± 8.9% vs 84.8 ± 0.4%), while meikin-N overexpression only had a slight effect on PBE (74.3 ± 3.8% vs 84.8 ± 0.4%) (Fig. 6e). The result indicates that the C-terminus is the important functional domain of MEIKIN.

To study the post-translational modification of MEIKIN, we applied Lambda Protein Phosphatase-λPPase to treat the MEIKIN overexpression oocytes to verify that MEIKIN underwent phosphorylation. The result showed that the molecular weight of Myc-MEIKIN in the MEIKIN overexpression oocytes at the GVBD stage was reduced to 70 kDa (consistent with the GV stage) with λPPase treatment, while the molecular weight was still 100 kDa without λPPase treatment (Fig. 6f). Similarly, the molecular weight of Myc-MEIKIN-C at the GVBD stage was reduced to 35 kDa (consistent with the GV stage) with λPPase treatment (Fig. 6g). Thus, these results indicate that the C-terminal region of MEIKIN undergoes phosphorylation after GVBD.

PLK1, but not CDK1, Aurora A/B, PKC, CK2, and MAPK, is involved in the phosphorylation of MEIKIN

A recent study reported that MEIKIN interacts with PLK1 (Kim et al. 2015; Miyazaki et al. 2017), a key kinase in meiosis (Ito et al. 2008; Tong et al. 2002; Xiong et al. 2008). Therefore, we speculated that PLK1 might be involved in the phosphorylation of MEIKIN. We applied BI6727, an inhibitor of PLK1, to treat the MEIKIN overexpression oocytes. Western blotting revealed that the molecular weight of Myc-MEIKIN in MEIKIN overexpression oocytes at the GVBD stage was reduced with BI6727 treatment, while the molecular weight was still 100 kDa with DMSO treatment. Thus, PLK1 was involved in the phosphorylation of MEIKIN (Fig. 7a).

We then explored whether other important meiotic cell cycle-related kinases, including CDK1, Aurora A/B, PKC, CK2, and MAPK, were involved in the phosphorylation of MEIKIN. We applied respectively the inhibitor

of CDK1—roscovitine, the inhibitor of Aurora A/B—ZM447439, the inhibitor of PKC—LY317615, the siRNA of PKC—*siPkc*, the inhibitor of CK2—TBB, and the inhibitor of MAPK—VX702, to treat the MEIKIN overexpression oocytes. The results showed that roscovitine, ZM447439, LY317615, *siPKC*, TBB, or VX702 did not cause the reduction of Myc-MEIKIN molecular weight at the GVBD stage (Fig. 7b–f). These results confirm that CDK1, Aurora A/B, PKC, CK2, and MAPK are not involved in the phosphorylation of meikin.

Discussion

It was reported previously that MEIKIN shows specific expression only in the ovary and testis. MEIKIN is localized at centromeres in meiotic oocytes and spermatocytes, and it disappears from the centromeres during the MII stage. MEIKIN recruits Shugoshin and PLK1 to centromeres, regulates the mono-orientation of sister kinetochores at the MI stage, and protects cohesin complexes at centromeres. Knockout of MEIKIN causes complete infertility in both male and female mice. Male meikin mutant mice show disrupted meiotic spermatogenesis and failure to produce mature sperm. Female meikin mutant mice can produce normal GV oocytes and these GV oocytes can be cultured to the GVBD stage in vitro; however, the first polar body extrusion is delayed by 2 h (Kim et al. 2015). Live-cell imaging also shows that sister kinetochores and sister chromatids separate prematurely in *Meikin*$^{-/-}$ oocytes and chromosomes misalign at the MII stage following the loss of localization of Rec8 and cohesin complexes at centromeres. The present study further investigated the function of MEIKIN in oocyte meiotic maturation and activation by employing a series of cellular and biochemical approaches and revealed some novel findings.

We first studied the expression pattern of MEIKIN during mouse oocyte meiotic maturation and early embryonic development. We found that meikin is a maternal factor and its mRNA was reduced in MII-stage mature oocytes, and abruptly decreased in fertilized eggs, and its specific expression pattern may be critical for oocyte meiotic maturation and early embryonic development. We also examined the accurate localization of MEIKIN by injecting exogenous *Myc-Meikin* mRNA into oocytes and further determined its localization by monoclonal Myc antibody staining which has been confirmed to be highly specific and effective in our previous studies (Qi et al. 2015, 2013; Zhang et al. 2015). Our results showed that MEIKIN was strongly accumulated around centromeres of chromosomes in meiosis I, but its staining was faint at the MII stage.

Next, we further studied the function of MEIKIN in oocyte meiotic maturation. Although previous studies have found that MEIKIN can regulate the mono-orientation of sister kinetochores in oocytes and protect the Rec8–cohesin complexes at centromeres by way of gene knockout (Kim et al. 2015), we still do not know the detailed function and the mechanism of MEIKIN function in the meiotic progression process. MEIKIN expression is decreased with oocyte maturation and fertilization. We injected exogenous *Myc-Meikin* mRNA to clarify the biological significance of reduced expression in mature oocyte and fertilized egg. Strikingly, exogenous expression of Myc-MEIKIN in GV oocytes caused MI arrest, which was unexpected taking consideration of the previously reported function of MEIKIN. The knockout of MEIKIN caused a delay of PBE and previous segregation of sister chromatids (Kim et al. 2015); so overexpression of MEIKIN should not affect or should even promote PBE and prevent the precocious segregation of sister chromatids. However, our results showed that expression of exogenous MEIKIN strongly inhibited PBE; even the culture time was prolonged, and oocytes could not break the MI arrest to extrude the first polar body. Moreover, we also found that overexpression of Myc-MEIKIN in MII oocytes prevented the second meiosis resumption and parthenogenetic activation of oocytes. Overexpression of MEIKIN in zygotes inhibited early cleavage and significantly reduced early embryonic development. Therefore, our results further revealed some novel functions of MEIKIN in regulating oocyte meiotic cell cycle progression and early embryo development.

Our subsequent studies found that overexpression of Myc-MEIKIN caused chromosome misalignments and activated SAC at the MI stage. Thus, SAC activation might be one of the reasons for the MI arrest. But our rescue experiment showed that the treatment of AZ3146 (an Mps1 inhibitor) or the depletion of Mad2 did not significantly rescue the MI arrest caused by exogenous MEIKIN expression. The result suggests that chromosome misalignment and SAC activation caused by exogenous MEIKIN expression may be one of the reasons for the MI arrest, but it is not the only reason and not the main reason.

Then we investigated the expression of cyclin B1 and Securin in oocytes, which are directly related to the metaphase–anaphase transition (Clute and Pines 1999; Peters 2006). We found that exogenous MEIKIN expression inhibited the degradation of cyclin B1 and Securin, which caused the high expression of cyclin B1 and Securin and then inhibited homologous chromosome separation and anaphase onset. We also found that treatment with roscovitine (a CDK inhibitor) or the depletion of Securin both significantly rescued the MI arrest caused by overexpressed MEIKIN.

We further investigated the detailed molecular mechanism of the MI arrest caused by exogenous MEIKIN expression. In our experiments, we unexpectedly observed that the molecular weight of Myc-MEIKIN changed after GVBD; it

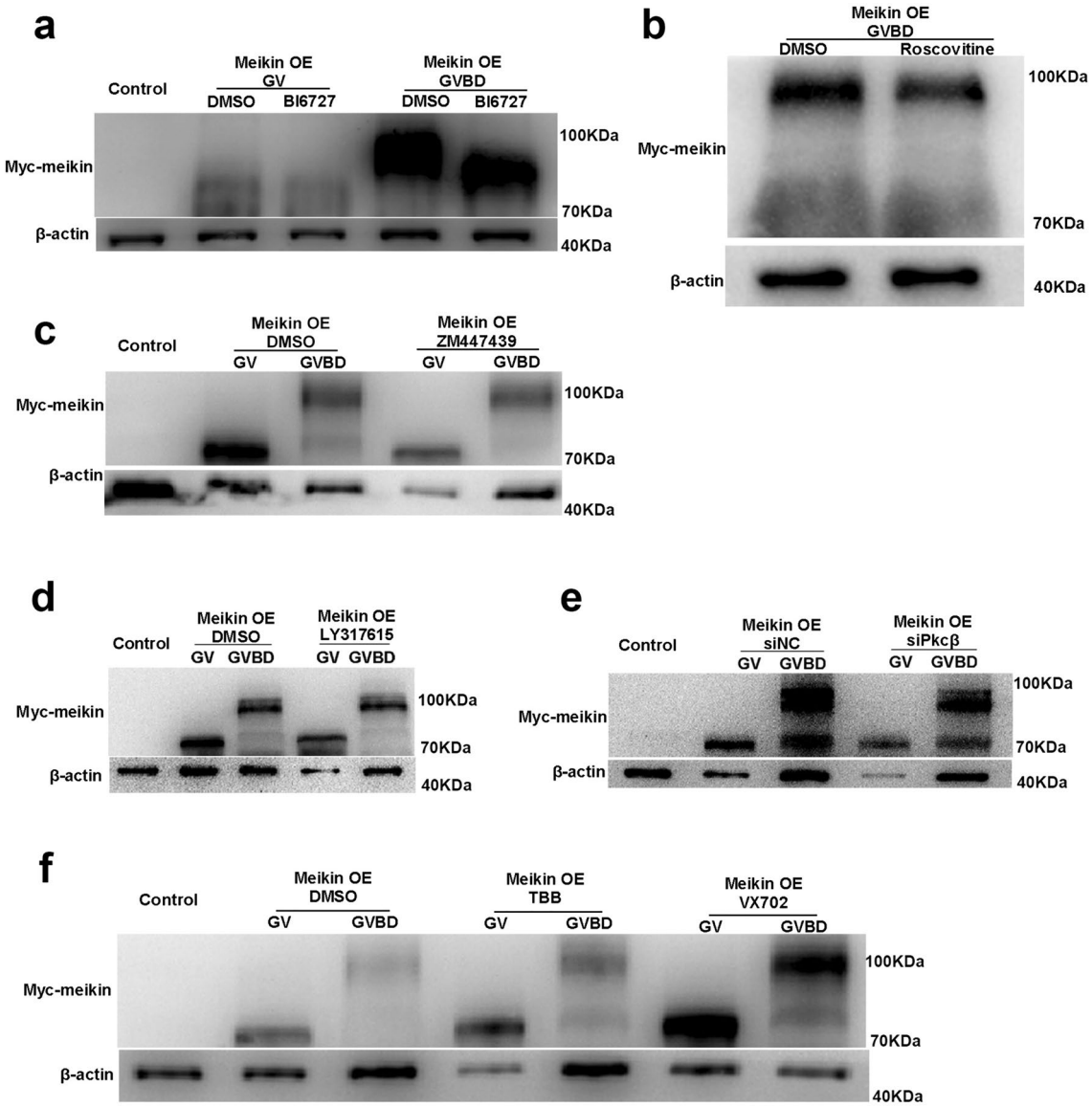

Fig. 7 PLK1, but not CDK1, Aurora A/B, PKC, CK2, and MAPK, is involved in the phosphorylation of MEIKIN. **a** The expression change of Myc-MEIKIN after BI6727 treatment. The oocytes with overexpressed MEIKIN were cultured in a medium containing 200 nM BI6727 or the same dose of DMSO for 14 h. A total of 50 oocytes were used in each lane for western blotting, and the level of β-actin was used as an internal control. **b** The expression changes of Myc-MEIKIN after roscovitine treatment. The oocytes with overexpressed MEIKIN were cultured in a medium containing 200 μM roscovitine or the same dose of DMSO for 14 h. **c** The expression changes of Myc-MEIKIN after ZM447439 treatment. The oocytes with overexpressed MEIKIN were cultured in a medium containing 5 μM ZM447439 or the same dose of DMSO for 14 h. **d** The expression changes of Myc-MEIKIN after LY317615 treatment. The oocytes with overexpressed MEIKIN were cultured in a medium containing 50 μM LY317615 or the same dose of DMSO for 14 h. **e** The expression changes of Myc-MEIKIN after PKC RNAi. *Myc-Meikin* mRNA (1 μg/μl) plus *Pkc* siRNA (*siPkc*, 30 μM) or the same dose control *siRNA* (*siCon*) was injected into the GV oocytes, and the oocytes were inhibited for 24 h with IBMX. Then the oocytes were released and cultured for 14 h. **f** The expression changes of Myc-MEIKIN after TBB or VX702 treatment. The oocytes with overexpressed MEIKIN were cultured in a medium containing 50 μM TBB or VX702 and the same dose of DMSO for 14 h

increased approximately to 30 kDa compared with that at the GV stage. However, Maier et al. (2021) found that Separase could cleave MEIKIN at anaphase I transition, which was inconsistent with our result. We inferred that Myc-MEIKIN might exert a new function and undergo post-translational modification after GVBD, and this post-translational modification might be related to its specific expression pattern and function. Because the localization of MEIKIN at the centromeres was significantly weakened or even completely disappeared at the MII stage and overexpression of MEIKIN inhibited the ubiquitinated degradation of cyclin B1 and Securin, we hypothesized that MEIKIN might underdo

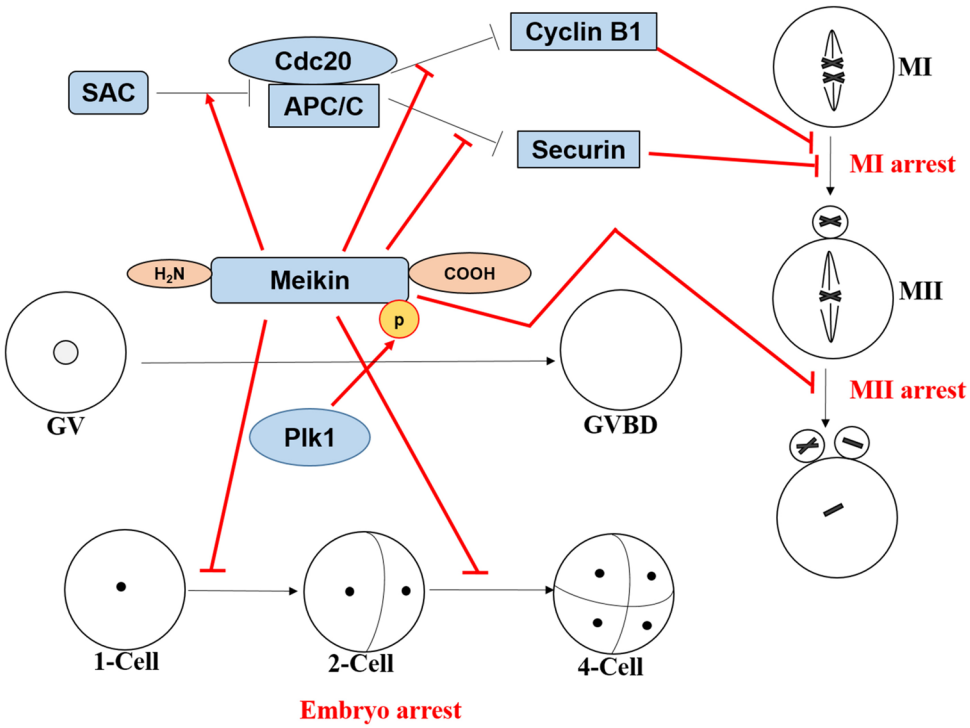

Fig. 8 The underlying mechanisms of MEIKIN regulation in meiosis. MEIKIN was a maternal protein phosphorylated by PLK1 at its carboxyl terminal region after GVBD, and the C-terminus was its key functional domain. Exogenous expression of MEIKIN resulted in chromosome misalignment, cyclin B1 and Securin degradation failure, and MI arrest through a SAC-independent mechanism. Exogenous expression of MEIKIN also inhibited MII exit and early embryo development

ubiquitinated degradation at the metaphase–anaphase transition. Moreover, previous reports showed that MEIKIN could interact with the *Ubb* gene in a yeast two-hybridization test (Kim et al. 2015), and the coding gene of polyubiquitin, *Ubb*, encoded four ubiquitin polypeptides with a molecular weight of about 30 kDa. In addition, it has been reported that the knockout of the *Ubb* gene in mice also led to infertility and meiosis arrest in oocytes and significantly inhibited PBE (Ryu et al. 2008). These results suggest that the post-translational modification of MEIKIN after GVBD may be the ubiquitinated modification. Overexpressed MEIKIN may competitively bind ubiquitin, thus inhibiting the normal ubiquitinated degradation of cyclin B1 and Securin to cause the MI arrest. To provide evidence to support the hypothesis, we investigated whether MEIKIN is the direct substrate of APC/C. We treated MEIKIN overexpressed oocytes with TAME (the APC/C inhibitor), and showed that TAME treatment did not rescue the post-translational modification of MEIKIN, indicating that MEIKIN is not the direct substrate of APC/C.

In addition, we divided MEIKIN protein (434 aa) into MEIKIN -N (1-300 aa) and MEIKIN-C (301-434 aa) and overexpressed respectively MEIKIN -N and MEIKIN-C in the oocytes. We found that the molecular weight of Myc-MEIKIN-N did not change after GVBD; however, the molecular weight of Myc-MEIKIN-C increased after GVBD. The result suggests that the post-translational modification of MEIKIN occurs in its C-terminus. We further studied the effects of MEIKIN-N and MEIKIN-C overexpression on oocyte meiotic maturation, and found that MEIKIN-N overexpression had only a slight effect on PBE, while MEIKIN-C overexpression strongly inhibited PBE. These results indicate that MEIKIN-C is the important functional domain of MEIKIN. Our conclusion was supported by a previous study, which showed that the localization of MEIKIN was dependent on the C-terminus (Kim et al. 2015).

Since meikin was not the direct substrate of APC/C, the post-translational modification of MEIKIN might not be ubiquitination. Because phosphorylation plays an important role in meiotic cell cycle progression, we examined whether MEIKIN undergoes phosphorylation. We applied λPPase to treat the MEIKIN overexpression oocytes and showed that λPPase treatment could rescue the post-translational modification of MEIKIN in the MEIKIN or MEIKIN-C overexpressed oocytes, indicating that the C-terminal region of MEIKIN undergoes phosphorylation.

Then we further clarified which protein kinases caused MEIKIN phosphorylation. We tested several important kinases regulating the meiotic cell cycle, including CDK1, Aurora A/B, PKC, CK2, and MAPK, and found that none of them is involved in the phosphorylation of MEIKIN. The literature reported that MEIKIN interacts with PLK1 and recruits PLK1 to centromeres (Kim et al. 2015; Miyazaki et al. 2017), and PLK1 is a key kinase in meiotic cell cycle regulation as previously reported by others and us (Ito et al. 2008; Tong et al. 2002; Xiong et al. 2008). Therefore, we speculated that PLK1 might be involved in the phosphorylation of MEIKIN. Then we applied BI6727 (the inhibitor

of Plk1) to treat the MEIKIN overexpression oocytes and revealed that BI6727 could rescue the phosphorylation of MEIKIN. Thus, PLK1 is involved in the phosphorylation of MEIKIN in meiotic oocyte.

In conclusion, our present study shows a novel function of MEIKIN in regulating the degradation of cyclin B and Securin during the metaphase–anaphase transition through PLK1-mediated phosphorylation (Fig. 8), besides its well-known roles in the regulation of sister chromatid mono-orientation and centromeric cohesion protection. Because of the unavailability of the antibody that recognizes MEIKIN, our study was mainly based on exogenous expression of MEIKIN, which did not entirely reflect the function of MEIKIN protein under physiological conditions, but the findings reveal the biological significance of reduced expression of MEIKIN during later stages of oocyte meiotic maturation and early embryo development. We tried to apply mass spectrometry to detect the phosphorylated residues of MEIKIN and the direct interaction between PLK1 and MEIKIN. However, because of the limited number of oocytes and the low level of MEIKIN protein, we did not adequately clarify these questions. In addition, how MEIKIN affects cyclin B and Securin levels needs further clarification.

Conclusion

Our study shows that MEIKIN expression and its C-terminal phosphorylation mediated by PLK1 are critical for regulating the metaphase–anaphase transition of the first meiosis and exit of the second meiosis via affecting the degradation of cyclin B1 and Securin in meiotic oocytes (Fig. 8). This study may have important guiding value for the prevention and treatment of infertility caused by oocyte meiotic abnormality.

Supplementary Information The online version contains supplementary material available at https://doi.org/10.1007/s00418-024-02316-7.

Acknowledgements We thank Li-Juan Wang for assistance with live cell imaging and Shi-Wen Li and Xi-Li Zhu for assistance with immunofluorescence staining. We thank Prof. Heng-Yu Fan of Zhejiang University and Dr. Jun-Yu Ma at Guangdong Second Provincial General Hospital for supply with GFP-Ccnb1and mCherry-Securin plasmids. We thank the other members in Prof. Sun's laboratory for their kind technical assistance and discussions. We are thankful for the funding provided by National R&D Program of China and National Natural Science Foundation of China.

Author contributions L.-H. Fan, S.-T. Qi, X.-H. Ou, W.-H. Wang and Q.-Y. Sun conceived and designed the project. L.-H. Fan, S.-T. Qi, Z.-B. Wang, Y.-C. Ouyang, W.-L. Lei, Y. Wang, A. Li., F. Wang and Y. Hou prepared and performed the experiments. L.-H. Fan, S.-T. Qi analyzed the data. J. Li., L. Li, Y.-Y. Li provided technical support and helped analyze the data. L.-H. Fan, S.-T. Qi, H. Schatten, X.-H. Ou, W.-H. Wang and Q.-Y. Sun prepared the paper. All authors approved the final version of the manuscript.

Funding This research was supported by National Natural Science Foundation of China (no. 32300952 and no. 32230028), and Guangdong Basic and Applied Basic Research Foundation (no. 2023B1515120027).

Data availability The data and material during the current study are available from the corresponding author on reasonable request.

Declarations

Conflict of interest The authors declare no competing interests.

Ethics approval and consent to participate All animal experiments conformed to the animal ethics of the Guangdong Second Provincial General Hospital and the Institute of Zoology, Chinese Academy of Sciences.

Consent for publication The authors agree to publication in the *Histochemistry and Cell Biology*.

References

Clute P, Pines J (1999) Temporal and spatial control of cyclin B1 destruction in metaphase. Nat Cell Biol 1:82–87

Fan L-H, Wang Z-B, Li Q-N, Meng T-G, Dong M-Z, Hou Y, Ouyang Y-C, Schatten H, Sun Q-Y (2019) Absence of mitochondrial DNA methylation in mouse oocyte maturation, aging and early embryo development. Biochem Biophys Res Commun 513:912–918

Hassold T, Hunt P (2001) To err (meiotically) is human: the genesis of human aneuploidy. Nat Rev Genet 2:280–291

Hodges CA, Hunt PA (2002) Simultaneous analysis of chromosomes and chromosome-associated proteins in mammalian oocytes and embryos. Chromosoma 111:165–169

Ito J, Yoon S-Y, Lee B, Vanderheyden V, Vermassen E, Wojcikiewicz R, Alfandari D, De Smedt H, Parys JB, Fissore RA (2008) Inositol 1,4,5-trisphosphate receptor 1, a widespread Ca^{2+} channel, is a novel substrate of polo-like kinase 1 in eggs. Dev Biol 320:402–413

Jones KT, Lane SI (2013) Molecular causes of aneuploidy in mammalian eggs. Development 140:3719–3730

Katis VL, Matos J, Mori S, Shirahige K, Zachariae W, Nasmyth K (2004) Spo13 facilitates monopolin recruitment to kinetochores and regulates maintenance of centromeric cohesion during yeast meiosis. Curr Biol 14:2183–2196

Kim J, Ishiguro K-I, Nambu A, Akiyoshi B, Yokobayashi S, Kagami A, Ishiguro T, Pendas AM, Takeda N, Sakakibara Y, Kitajima TS, Tanno Y, Sakuno T, Watanabe Y (2015) Meikin is a conserved regulator of meiosis-I-specific kinetochore function. Nature 517:466–471

Lee JY, Orr-Weaver TL (2001) The molecular basis of sister-chromatid cohesion. Annu Rev Cell Dev Biol 17:753–777

Lee BH, Kiburz BM, Amon A (2004) Spo13 maintains centromeric cohesion and kinetochore coorientation during meiosis I. Curr Biol 14:2168–2182

Li J, Qian WP, Sun QY (2019) Cyclins regulating oocyte meiotic cell cycle progression†. Biol Reprod 101:878–881

Maier NK, Ma J, Lampson MA, Cheeseman IM (2021) Separase cleaves the kinetochore protein Meikin at the meiosis I/II transition. Dev Cell 56:2192-2206.e2198

Marston AL, Amon A (2004) Meiosis: cell-cycle controls shuffle and deal. Nat Rev Mol Cell Biol 5:983–997

Mihajlović AI, FitzHarris G (2018) Segregating chromosomes in the mammalian oocyte. Curr Biol 28:R895-r907

Miyazaki S, Kim J, Yamagishi Y, Ishiguro T, Okada Y, Tanno Y, Sakuno T, Watanabe Y (2017) Meikin-associated polo-like kinase specifies Bub1 distribution in meiosis I. Genes Cells Devoted Mol Cell Mech 22:552–567

Musacchio A, Salmon ED (2007) The spindle-assembly checkpoint in space and time. Nat Rev Mol Cell Biol 8:379–393

Peters J-M (2006) The anaphase promoting complex/cyclosome: a machine designed to destroy. Nat Rev Mol Cell Biol 7:644–656

Petronczki M, Siomos MF, Nasmyth K (2003) Un ménage à quatre: the molecular biology of chromosome segregation in meiosis. Cell 112:423–440

Qi S-T, Wang Z-B, Ouyang Y-C, Zhang Q-H, Hu M-W, Huang X, Ge Z, Guo L, Wang Y-P, Hou Y, Schatten H, Sun Q-Y (2013) Overexpression of SETβ, a protein localizing to centromeres, causes precocious separation of chromatids during the first meiosis of mouse oocytes. J Cell Sci 126:1595–1603

Qi S-T, Wang Z-B, Huang L, Liang L-F, Xian Y-X, Ouyang Y-C, Hou Y, Sun Q-Y, Wang W-H (2015) Casein kinase 1 (α, δ and ε) localize at the spindle poles, but may not be essential for mammalian oocyte meiotic progression. Cell Cycle 14:1675–1685

Ryu K-Y, Sinnar SA, Reinholdt LG, Vaccari S, Hall S, Garcia MA, Zaitseva TS, Bouley DM, Boekelheide K, Handel MA, Conti M, Kopito RR (2008) The mouse polyubiquitin gene Ubb is essential for meiotic progression. Mol Cell Biol 28:1136–1146

Sullivan M, Morgan DO (2007) A novel destruction sequence targets the meiotic regulator Spo13 for anaphase-promoting complex-dependent degradation in anaphase I. J Biol Chem 282:19710–19715

Sun SC, Kim NH (2012) Spindle assembly checkpoint and its regulators in meiosis. Hum Reprod Update 18:60–72

Tong C, Fan H-Y, Lian L, Li S-W, Chen D-Y, Schatten H, Sun Q-Y (2002) Polo-like kinase-1 is a pivotal regulator of microtubule assembly during mouse oocyte meiotic maturation, fertilization, and early embryonic mitosis. Biol Reprod 67:546–554

Xiong B, Sun S-C, Lin S-L, Li M, Xu B-Z, OuYang Y-C, Hou Y, Chen D-Y, Sun Q-Y (2008) Involvement of Polo-like kinase 1 in MEK1/2-regulated spindle formation during mouse oocyte meiosis. Cell Cycle 7:1804–1809

Yokobayashi S, Watanabe Y (2005) The kinetochore protein Moa1 enables cohesion-mediated monopolar attachment at meiosis I. Cell 123:803–817

Zhang T, Zhou Y, Qi S-T, Wang Z-B, Qian W-P, Ouyang Y-C, Shen W, Schatten H, Sun Q-Y (2015) Nuf2 is required for chromosome segregation during mouse oocyte meiotic maturation. Cell Cycle 14:2701–2710